Journal of Alloys and Compounds 520 (2012) 180–189

Contents lists available at SciVerse ScienceDirect

Journal of Alloys and Compounds

journal homepage: www.elsevier.com/locate/jallcom

Structural features of two novel alluaudite-like arsenates $Cd_{1.16}Zn_{2.34}(AsO_4)_{1.5}(HAsO_4)(H_2AsO_4)_{0.5}$ and $Cd_{0.74}Mg_{2.76}(AsO_4)_{1.5}(HAsO_4)(H_2AsO_4)_{0.5}$

Jovica Stojanović [a,*], Tamara Đorđević [b], Ljiljana Karanović [c]

[a] Institute for Technology of Nuclear and Other Mineral Raw Materials, Applied Mineralogy Unit, Franchet d'Esperey 86, P.O. Box 390, 11000 Belgrade, Serbia
[b] Institut für Mineralogie und Kristallographie, Geozentrum, Universität Wien, Althanstrasse 14, A-1090 Wien, Austria
[c] Laboratory of Crystallography, Faculty of Mining and Geology, University of Belgrade, Đušina 7, 11000 Belgrade, Serbia

ARTICLE INFO

Article history:
Received 5 October 2011
Received in revised form
26 December 2011
Accepted 1 January 2012
Available online 9 January 2012

Keywords:
Inorganic materials
Chemical synthesis
Crystal structure
X-ray diffraction

ABSTRACT

Two new compounds, $Cd_{1.16}Zn_{2.34}(AsO_4)_{1.5}(HAsO_4)(H_2AsO_4)_{0.5}$ (**1**) and $Cd_{0.74}Mg_{2.76}(AsO_4)_{1.5}(HAsO_4)(H_2AsO_4)_{0.5}$ (**2**), have been prepared hydrothermally. Their crystal structures consist of chains of edge-sharing $M1O_4(OH_{0.5})_2$, $M1aO_4(OH_{0.5})_2$, $M2O_5(OH_{0.5})$, and $M2aO_5(OH_{0.5})$ octahedra ($M1$, $M1a$ = Zn, Cd; $M2$, $M2a$ = Zn for **1**, and $M1$, $M1a$ = Mg, Cd; $M2$, $M2a$ = Mg for **2**) that are stacked parallel to (1 0 1) and are connected by the $[(AsO_4)_{0.5}(AsO_3(OH))_{0.5}]^{2.5-}$ and $[(AsO_4)_{0.5}(AsO_2(OH)_2)_{0.5}]^{2-}$ tetrahedra. These chains produce two types of channels parallel to the *c*-axis. Cd atoms are located in channels 2, while in channels 1 are situated hydrogen atoms of OH groups. The infrared spectra clearly show the presence of broad O—H stretching and bending vibrations centred at 3236, 2392 1575 and 1396 cm^{-1} in (**1**), and 3210, 2379 1602 and 1310 cm^{-1} in (**2**). The O—H stretching frequency is in good agreement with O···O distances. Furthermore, structural characteristics of compounds with similar alluaudite-like structures were discussed.

1. Introduction

The minerals of the alluaudite group and their synthetic counterparts show great compositional and structural variability. Up to date, about 90 natural and synthetic phosphate and arsenates, belonging to the alluaudite structure type were recognized [1–39 and references therein].

The natural alluaudites display chemical compositions varying between the two end-members, $Na_2Mn(Fe^{2+},Fe^{3+})(PO_4)_3$ and $\square NaMnFe_2{}^{3+}(PO_4)_3$, where □ is a vacancy [11]. Moore [40] had determined the crystal structure of alluaudite in the monoclinic $C2/c$ space group and yielded the general structural formula $X2X1M1M2_2(PO_4)_3$ (X are large cations, and M are distorted octahedral centres) with four formula units per unit cell. It represents the parental structure-type of the group referred to as 'alluaudite type'. Later, according to Leroux et al. [8], $X1$ and $X2$ have been relabeled to $A1$ and $A2$, respectively. In the structure of alluaudites the three-dimensional heteropolyhedral framework formed by PO_4 tetrahedra and MO_6 octahedra delimits two types of channels running along the *c*-axis. Channels 1 are slightly smaller and elongated in the *b*-direction, and channels 2 are slightly bigger and elongated in the *a*-direction. The large cation $A1$ is localized in channel 1 running along (½, 0, *z*), and (0, ½, *z*) (4*b* Wyckoff position in $C2/c$) and $A2$ lies in channel 2 running along (0, 0, *z*) and (½, ½, *z*) (4*a* Wyckoff position in $C2/c$). Hatert et al. [11,34] systematized literature data concerning a variety of alluaudite-like compounds and improved the cation site nomenclature. Besides $A1$ and $A2$ they recognized three new $A2'$, $A1'$, $A1''$ positions in $C2/c$ space group: $A2'$ corresponds to (0, *y*, ¼) with $y \approx 0$ in channel 2 (4*e* Wyckoff position), $A1'$ is localized on (0, *y*, ¼) with $y \approx ½$ in channel 1 (4*e* Wyckoff position), and $A1''$ site occurs on the general (*x*, *y*, *z*) position in channel 1 (8*f* Wyckoff position). The new general formula of the group proposed by Hatert et al. [11] is $[A2A2'][A1A1'A1''_2]M1M2_2[XO_4]_3$ ($X = P^{5+}$, As^{5+}), where A sites may be either vacant or partially filled, depending on the cation substitution. The small pentovalent cations X and large variable-valence cations $M1$ and $M2$ (mainly divalent and trivalent cations) are distributed over two tetrahedral and two octahedral sites, respectively.

A further structure variant was found in $Cd_{1.16}Zn_{2.34}(AsO_4)_{1.5}(HAsO_4)(H_2AsO_4)_{0.5}$ (**1**) and $Cd_{0.74}Mg_{2.76}(AsO_4)_{1.5}(HAsO_4)(H_2AsO_4)_{0.5}$ (**2**) during an ongoing research on heteropolyhedral framework structures of divalent metal phosphates and arsenates with potentially interesting structural, physical and chemical properties [41–46].

The present contribution reports the hydrothermal synthesis and crystal structures of the two previously unknown compounds.

---

[*] Corresponding author. Tel.: +381 11 3691 722; fax: +381 11 3691 583.
E-mail address: j.stojanovic@itnms.ac.rs (J. Stojanović).

0925-8388/$ – see front matter © 2012 Elsevier B.V. All rights reserved.
doi:10.1016/j.jallcom.2012.01.002

Table 1
Unit-cell parameters of alluaudite-like compounds having protonated arsenate and phosphate groups.

Chemical formula	a (Å)	b (Å)	c (Å)	β (°)	V (Å^3)	Reference
$AgNi_3(PO_4)(HPO_4)_2$	11.865(4)	12.117(3)	6.467(2)	113.82(3)	850.6(4)	[49]
$AgMg_3(PO_4)(HPO_4)_2$	11.9126(5)	12.1197(6)	6.4780(3)	113.812(2)	855.66(7)	[50]
$NaCo_3(PO_4)(HPO_4)_2$	11.865(2)	12.137(2)	6.512(1)	114.12(1)	855.9(2)	[5]
$AgCo_3(PO_4)(HPO_4)_2$	12.035(2)	12.235(2)	6.541(2)	114.14(2)	878.9(3)	[17]
$NaMn_3(PO_4)(HPO_4)_2$	12.179(2)	12.405(1)	6.6602(8)	114.616(7)	914.7(2)	[7]
$AgMn_3(PO_4)(HPO_4)_2$	12.263(1)	12.446(2)	6.649(1)	114.708(8)	921.9(2)	[8]
$Cd_{0.74}Mg_{2.76}(HAsO_4)(H_{0.5}AsO_4)_2$	11.992(2)	12.429(3)	6.746(1)	112.92(3)	926.1(4)	This study
$NaCo_3(AsO_4)(HAsO_4)_2$	12.054(1)	12.378(1)	6.780(2)	113.03(1)	931.0(3)	[5]
$AgCo_3(AsO_4)(HAsO_4)_2$	12.159(9)	12.438(7)	6.782(3)	113.2(0)	943.0	[47]
$Na(Zn,Mg)_3(AsO_4)(HAsO_4)_2$	12.113(3)	12.445(4)	6.793(1)	112.87(2)	943.5(4)	[48]
$AgZn_3(AsO_4)(HAsO_4)_2$	12.169(2)	12.495(3)	6.755(1)	112.8(0)	947.1	[47]
$Cd_{1.16}Zn_{2.34}(AsO_4)_{1.5}(HAsO_4)(H_2AsO_4)_{0.5}$	12.250(3)	12.491(3)	6.816(1)	113.62(3)	955.6(3)	This study
$NaMn_3(AsO_4)(HAsO_4)_2$	12.299(3)	12.735(3)	6.893(2)	113.587(4)	989.5(4)	[13]
$AgMn_3(AsO_4)(HAsO_4)_2$	12.397(2)	12.707(2)	6.8904(6)	113.57(1)	994.8(2)	[23]
$KMn_3(AsO_4)(HAsO_4)_2$	12.706(3)	12.731(3)	6.937(2)	113.175(5)	1031.6(4)	[13]

Furthermore, these compounds represent new structure types. During past three decades, 13 protonated phosphates and arsenates adopting alluaudite structure have been reported in the literature [5,7,8,13,17,23,47–50]. Similarly to **1** and **2** in all these structures hydrogen atoms are in $A1''$ general position situated in channel 1, while monovalent Ag, K, and Na cations are in channels 1 and 2, located in various A positions. Unit-cell parameters of alluaudite-like compounds having protonated arsenate and phosphate groups are given in Table 1.

2. Experimental

2.1. Sample preparation

Single crystals of the title compounds were synthesized hydrothermally from the mixtures of $Cd(OH)_2$ (Alfa Products 89297), $5ZnO{\cdot}2CO_3{\cdot}4H_2O$ (Alfa Products 308764), $3As_2O_5{\cdot}5H_2O$ (99%, Merck) in a molar ratio 1:1:1 for **1** and $Cd(OH)_2$ (Alfa Products 89297), MgO (>97%, Merck 5865), $3As_2O_5{\cdot}5H_2O$ (99%, Merck) in a molar ratio 1:2:1 for **2**. The initial pH of **1** and **2** were 5 and 6, respectively. The mixture for **1** was transferred into teflon vessel and filled up to approximately 70% of their inner volume with distilled water. The teflon vessels were enclosed in stainless steel autoclaves. The mixture was heated under autogeneous pressure from room temperature to 473 K (for 4 h), held at this temperature 72 h and finally cooled to room temperature 96 h. The mixture for **2** was heated under autogeneous pressure from room temperature to 493 K (for 4 h), held at this temperature 96 h and finally cooled to room temperature 96 h.

The resulting products were filtered off, washed thoroughly with distilled water and dried in the air at room temperature. The title compounds crystallized as regular colourless prismatic and lath-like crystals (yield > 50%) up to 100 mm in length (Fig. 1). In both syntheses, the residue represents white powders, which have not been studied.

2.2. Chemical analyses

Qualitative chemical analyses were performed using a JEOL JSM-6400 LV scanning electron microscope connected with a LINK energy-dispersive X-ray analysis (EDX) unit. The presence of Cd, Zn, As in the **1** and Cd, Mg, As in the **2** was confirmed in studied single-crystals.

2.3. Infrared measurements

In order to investigate the hydrous species polarized single-crystal infrared (IR) absorption spectroscopy was performed. The spectra of **1** and **2** were recorded using a Fourier-Transform IR spectrophotometer Bruker Tensor 27 FTIR instrument, equipped with mid-IR glowbar light source and KBr beam splitter, attached to a Hyperion 2000 FTIR microscope with liquid nitrogen-cooled mid-IR, broad-band MCT detector. A total of 128 scans were accumulated between 4000 and 550 cm^{-1} circular sample aperture 100 μm diameter and ATR 15× objective.

2.4. Single-crystal X-ray diffraction experiments

The crystal quality of several single crystals of **1** and **2** were checked with a Nonius Kappa CCD single-crystal four-circle diffractometer (Mo tube, graphite monochromator, CCD detector frame size: 621 × 576 pixels, binned mode), equipped with a 300 μm diameter capillary-optics collimator. Each one sample exhibiting sharp reflection spots was chosen for data collection. Single-crystal X-ray intensity data of **1** were collected on a Bruker-Nonius APEX-II diffractometer with a CCD-area detector, equipped with a graphite monochromator and using Mo Kα radiation ($\lambda = 0.71073$ Å). A complete sphere of reciprocal space (φ and ω scans) was measured (see Table 2 for details). The intensity data were processed with the Bruker-Nonius programme suite SAINT-Plus and corrected for Lorentz, polarization, background and absorption effects [51]. Single-crystal X-ray intensity data of **2** were collected on Nonius Kappa CCD single-crystal four-circle diffractometer (Mo tube, graphite monochromator, CCD detector frame size: 621 × 576 pixels, binned mode), equipped with a 300 μm diameter capillary-optics collimator. A complete sphere of reciprocal space (φ and ω scans) was measured at room temperature (see Table 2 for details). The intensity data were processed with the Nonius program suite DENZO-SMN [52] and corrected for Lorentz, polarization, and background effects and, by the multi-scan method, for absorption [52,53].

3. Results and discussion

3.1. Structure solution

From cell metrics and intensity distribution a close structural relationship with the 'alluaudite type' was expected. In the first step the crystal structures of **1** and **2** were refined starting from the atomic coordinates of $AgMn_3(AsO_4)(HAsO_4)_2$ [23] in the parental monoclinic space group $C2/c$. This attempt yielded positions of all atoms, but R-indices (all data) were very high, $R_1 = 0.051$, $wR_2 = 0.115$, and $R_1 = 0.064$, $wR_2 = 0.157$ for **1** and **2**, respectively. The refinement was poor: the second WGHT parameter was very high, many large correlation matrix elements were observed, and some oxygen atoms became 'non-positive-definite'. Furthermore, there were numerous reflections that violate the systematic absences and they were rejected because of systematic absence violations, indicating that no c-glide ($h0l$ with $l = 2n$) is present and that the symmetry is lower than $C2/c$. Possible subgroups of $C2/c$ without a c-glide are $C2$, $P2/n$, and $P2_1/n$. The presence of an n-glide ($h0l$ with $h + l = 2n$) is also contradicted by many reflections, leaving $C2$ as the only possible space group for these new compounds. Additionally, many reflections disagreed largely with the model and for the most disagreeable reflections F_o^2 was always greater than F_c^2, the factor K ($= \langle F_o^2 \rangle / \langle F_c^2 \rangle$) was very high for the reflections with low intensity indicating twinning.

Having all that in mind, a solving of the crystal structure was attempted with a lower space group. Monoclinic symmetry is maintained, however, the true space group was without an inversion centre ($C2$), and therefore some positions are split into two configurationally similar but crystallographically distinct sites: $4e$ is split in $2a$ and $2b$ sites, while the general position $8f$ is split in two general positions $4c$. Accordingly, the general formula for alluaudites crystallizing in a space group $C2$ ($Z = 4$) is $[A2A2'_{0.5}A2'a_{0.5}][A1A1'_{0.5}A1'a_{0.5}A1''_2]M1_{0.5}M1a_{0.5}M2M2a[X1O_4]_{0.5}[X1aO_4]_{0.5}[X2O_4][X2aO_4]$. The asymmetric unit with the atom-numbering scheme is shown in Fig. 2.

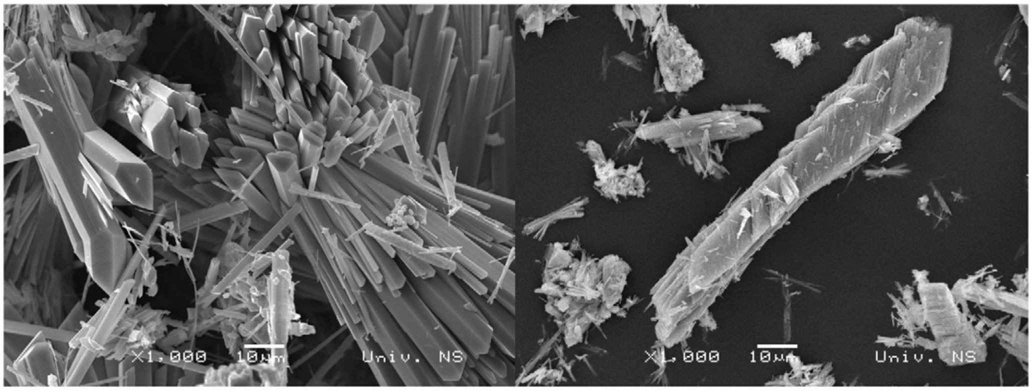

Fig. 1. Scanning electron micrographs of **1** (left) and **2** (right) crystals.

Changing to the correct space group *C*2 and taking into account racemic twinning significantly improved the refinement. The *R* values dropped to 0.021 and 0.022 (R_1) as well as 0.041 and 0.053 (wR_2) for **1** and **2**, respectively. It was necessary to introduce restraints for the atoms in the mixed $[M1]_{2b}$ and $[M1a]_{2a}$ sites, which were refined with the same coordinates and displacement parameters for Zn/Cd and Mg/Cd in **1** and **2**, respectively. For Cd atoms in channel 2 successive refinements were performed in which the occupancy of each Cd site, $[A2']_{2b}$ and $[A2'a]_{2a}$, was allowed to vary independently. These refinements showed that the sum of two occupancy factors is very close to 0.5 in both structures. Therefore, in the final run, the occupancy factors for Cd2 and Cd2*a* was refined with a fixed sum of occupancy factors of 0.5, *i.e.* restrains $\mathrm{Cd2}_x + \mathrm{Cd2}a_{0.5-x}$ were used. Additionally, these Cd atoms were refined with identical anisotropic displacement parameters. All H atoms were found in a difference Fourier map and successfully refined as riding atoms, with restraints on the O—H bond distances of 0.82 (2) Å and $U_{\mathrm{iso}}(\mathrm{H})$ values at $1.2U_{\mathrm{eq}}(\mathrm{O})$. Hydrogen atoms were found in general positions near to $[A1']_{2b}$ and $[A1'a]_{2a}$ positions and their occupancy factors were fixed at 0.5 in order to retain charge balance.

Both crystal structures were solved using direct methods with the SIR97 [54]. For the crystal structure refinement SHELXL97 [55] program within the WinGX [56] software package was used. The resulting crystallographic parameters for **1** and **2** are shown in Table 2. Fractional atomic coordinates, equivalent isotropic displacement and anisotropic displacement parameters for both compounds are given in Tables 3–6. Selected interatomic distances of both structures are summarized in Table 7. Bond valence sum calculations were obtained using *VALIST* software [57] and are shown

Table 2
Crystallographic data, data collection and refinement details for **1** and **2**.

Crystal data		
Chemical formula	$Cd_{1.16}Zn_{2.34}(AsO_4)_{1.5}(HAsO_4)(H_2AsO_4)_{0.5}$	$Cd_{0.74}Mg_{2.76}(AsO_4)_{1.5}(HAsO_4)(H_2AsO_4)_{0.5}$
Formula mass (amu)	706.36	569.26
Space group (No.)	*C*2 (5)	*C*2 (5)
α (Å)	12.250(3)	11.992(2)
b (Å)	12.491(3)	12.429(3)
c (Å)	6.816(1)	6.7462(13)
β (°)	113.62(3)	112.92(3)
V (Å^3)	955.6(4)	926.1(4)
Z	4	4
$\rho_{\mathrm{calc.}}$ (g cm^{-3})	4.880	4.083
Crystal dimensions (mm)	0.08 × 0.03 × 0.03	0.08 × 0.03 × 0.03
μ (cm^{-1})	18.74	12.68
Transmission fractors	0.514–0.570	0.640–0.684
Data collection		
Crystal-detector distance (mm)	36	36
Rotation width (°)	2	2
Total no. of frames	393	506
Collection time per frame (s)	300	160
h, k, l ranges	$-13 \le h \le 15$, $-15 \le k \le 15$, $-8 \le l \le 8$	$-14 \le h \le 14$, $-15 \le k \le 15$, $-8 \le l \le 8$
No. of data measured	5560	2205
No. of unique data, including $F_o^2 < 0$	1960	1895
No. of unique data, with $F_o^2 > 2\theta(F_o^2)$	1787	1090
Refinement		
No. of parameters	149	149
Number of restraints	1	1
$R(F)$ for $F_o^2 > 2\theta(F_o^2)$	0.021	0.022
$R_w(F_o^2)$[a]	0.041	0.053
Extinction coefficient, k[b]	0.0002(1)	0.0006(2)
Goodness of fit	1.07	1.13
Flack parameter	0.50(2)	0.58(2)
$(\Delta\rho)_{\max}$, $(\Delta\rho)_{\min}$ (e Å^{-3})	0.75, −1.44	0.45, −0.68

[a] $w = 1/[\sigma^2(F_o^2) + (0.0128P)^2 + 3.9527P]$ for **1**, and $w = 1/[\sigma^2(F_o^2) + (0.0207P)^2 + 6.6662P]$ for **2**, where $P = (F_o^2 + 2F_c^2)/3$.

[b] $F_c^* = kF_c[1 + 0.001F_c^2\lambda^3/\sin(2\theta)]^{-1/4}$.

Table 3
Fractional atomic coordinates and isotropic or equivalent isotropic displacement parameters for **1**. U_{eq} according to Fischer and Tillmanns [59]. For the H atoms U_{iso} is shown.

Atom	x	y	z	U_{iso}/U_{eq} (Å^2)	Occ. (<1)
Cd2	½	0.4731(8)	½	0.0390(3)	0.214(2)
Cd2*a*	½	0.5186(2)	0	0.0390(3)	0.787(2)
Zn1/Cd1	0	0.2811(1)	½	0.0130(3)	0.144(9)/0.856(9)
Zn1*a*/Cd1*a*	0	0.7139(1)	0	0.0115(4)	0.545(9)/0.455(9)
Zn2	0.2110(1)	0.1612(1)	0.3756(1)	0.0145(3)	
Zn2*a*	0.2029(1)	0.8441(1)	−0.1358(2)	0.0117(2)	
As1	0	0.3074(1)	0	0.0112(3)	
As1*a*	0	0.6917(1)	½	0.0072(3)	
As2	0.2838(1)	0.3900(1)	0.6388(1)	0.0093(2)	
As2*a*	0.2790(1)	0.6141(1)	0.1305(1)	0.0097(2)	
O1	0.0370(5)	0.2292(5)	0.2173(8)	0.015(1)	
O1*a*	0.0366(5)	0.7655(5)	−0.2787(7)	0.011(1)	
O2	0.1136(1)	0.3891(2)	0.0098(2)	0.010(1)	
H2	0.0931	0.4518	0.0069	0.013	
O2*a*	0.1114(1)	0.6084(2)	−0.4895(2)	0.017(1)	
H2*a*	0.0923	0.5463	−0.4797	0.020	
O3	0.3483(1)	0.3271(2)	0.8751(2)	0.013(1)	
O3*a*	0.3354(1)	0.6778(2)	0.3654(2)	0.015(1)	
O4	0.1380(1)	0.4164(2)	0.5861(2)	0.013(1)	
H4	0.1251	0.4806	0.5628	0.015	
O4*a*	0.1308(1)	0.5860(2)	0.0752(2)	0.019(1)	
H4*a*	0.1225	0.5214	0.08519	0.023	
O5	0.2877(1)	0.3176(2)	0.4353(2)	0.010(1)	
O5*a*	0.2839(1)	0.6896(2)	−0.0683(2)	0.014(1)	
O6	0.3543(1)	0.5068(2)	0.6657(2)	0.017(1)	
O6*a*	0.3530(1)	0.4993(2)	0.1423(2)	0.020(1)	

in Table 8. Hydrogen bonding geometry for both compounds is summarized in Table 9. Drawings of structural details were produced using the *ATOMS* software [58].

3.2. Description of the crystal structures

In **1** and **2** Cd ions partly occupy $[A2']_{2b}$ and $[A2'a]_{2a}$ sites in channels 2, as well as two mixed octahedral sites $[M1]_{2b}$ and $[M1a]_{2a}$ ($M1$ = Cd/Zn and Cd/Mg in **1** and **2**, respectively). The Zn in **1** and Mg in **2** fill two octahedral $[M2]_{4c}$ and $[M2a]_{4c}$ sites, while the four As atoms exhibit the usual tetrahedral coordination. Two As atoms are in special $[X1]_{2a}$ and $[X1a]_{2b}$, and two are in general $[X2]_{4c}$ and $[X2a]_{4c}$ positions.

The core of the structure is curved chain of variously distorted edge-sharing octahedra running in the $[1\,0\,\bar{1}]$ direction (Fig. 3). The chains contain edge-sharing $M2M2aO_8(OH_{0.5})_2$ octahedral pairs, which further share opposite edges with adjacent $M1O_4(OH_{0.5})_2$ and $M1aO_4(OH_{0.5})_2$ octahedra. Each As, situated in slightly deformed tetrahedron, shares common O atoms and OH groups from octahedral chains and link them in a layers which are normal to the *b*-axis (Fig. 4). There are two such layers per unit cell. The adjacent half-unit-cell layers are linked sharing common oxygen atoms (O6 and O6*a*) to form a heteropolyhedral 3D framework which generates two crystallographically distinct types of parallel channels along [0 0 1].

The cross-section of the channel 1 is a flattened hexagon with O2, O2*a*, O4, O4*a*, O6 and O6*a* atoms at their vertices. The $[A1]_{4c}$ site in *C*2 (corresponds to $[A1]_{4b}$ site in *C*2/*c*) is in the centre of the hole, while $[A1']_{2b}$ and $[A1'a]_{2a}$ sites are at centres of upper and lower basal planes (Fig. 5). The channel 2 can be described as a sequence of pairs of antiprisms, sharing common bases, *i.e.* two O6 and two O6*a* atoms. In the vertices of antiprisms are in hydrogen bonding

Table 4
Anisotropic displacement parameters for **1** with estimated standard deviation in parentheses. The anisotropic displacement parameters are defined as: $\exp[-2\pi^2\sum_{i=1}^{3}\sum_{j=1}^{3}U_i a_i^* a_j^* h_i h_j]$.

Atom	U_{11}	U_{22}	U_{33}	U_{23}	U_{13}	U_{12}
Cd2/Cd2*a*	0.0109(4)	0.0911(9)	0.0120(4)	0	0.0015(3)	0
Zn1/Cd1	0.0114(5)	0.0164(6)	0.0127(5)	0	0.0062(4)	0
Zn1*a*/Cd1*a*	0.0091(6)	0.0145(7)	0.0120(6)	0	0.0055(4)	0
Zn2	0.0193(5)	0.0127(5)	0.0148(5)	0.0015(5)	0.0103(4)	0.0031(5)
Zn2*a*	0.0152(5)	0.0093(5)	0.0134(5)	−0.0026(4)	0.0086(4)	−0.0013(4)
As1	0.0129(6)	0.0135(7)	0.0058(6)	0	0.0022(5)	0
As1*a*	0.0098(6)	0.0037(7)	0.0071(6)	0	0.0022(5)	0
As2	0.0126(4)	0.0069(4)	0.0085(4)	−0.0005(3)	0.0042(4)	0.0008(3)
As2*a*	0.0133(4)	0.0092(5)	0.0076(4)	−0.0018(4)	0.0051(4)	−0.0021(4)
O1	0.013(3)	0.021(4)	0.009(3)	0.003(3)	0.001(2)	−0.001(5)
O1*a*	0.013(2)	0.015(3)	0.008(2)	−0.007(2)	0.005(2)	−0.003(3)
O2	0.012(3)	0.003(3)	0.020(3)	0.004(2)	0.009(2)	0.001(2)
O2*a*	0.013(3)	0.016(3)	0.017(3)	0.001(3)	−0.001(2)	0.017(1)
O3	0.011(3)	0.009(3)	0.003(2)	0.005(2)	0.007(2)	0.013(1)
O3*a*	0.023(3)	0.014(3)	0.009(3)	−0.002(2)	0.008(2)	−0.002(2)
O4	0.013(3)	0.007(3)	0.020(3)	0.002(3)	0.007(2)	0.002(2)
O4*a*	0.012(3)	0.019(3)	0.028(3)	0.001(3)	0.010(2)	−0.001(3)
O5	0.013(3)	0.010(3)	0.008(3)	−0.002(2)	0.005(2)	0.001(2)
O5*a*	0.012(3)	0.020(3)	0.008(2)	−0.000(2)	−0.003(2)	−0.000(3)
O6	0.013(2)	0.008(3)	0.024(2)	0.008(2)	0.001(2)	−0.001(2)
O6*a*	0.016(2)	0.018(3)	0.025(2)	−0.006(3)	0.007(2)	0.020(1)

Table 5
Fractional atomic coordinates and isotropic or equivalent isotropic displacement parameters for **2**. U_{eq} according to Fischer and Tillmanns [63]. For the H atoms U_{iso} is shown.

Atom	x	y	z	U_{iso}/U_{eq} (Å^2)	Occ. (<1)
Cd2	½	0.509(2)	½	0.360(4)	0.096(2)
Cd2*a*	½	0.5053(2)	0	0.360(4)	0.904(2)
Mg1/Cd1	0	0.2806(3)	½	0.018(1)	0.674(5)/0.326(5)
Mg1*a*/Cd1*a*	0	0.7152(3)	0	0.015(1)	0.841(6)/0.159(5)
Mg2	0.2078(3)	0.1657(4)	0.3708(5)	0.008(1)	
Mg2*a*	0.2006(3)	0.8460(4)	−0.1419(6)	0.010(1)	
As1	0	0.3131(1)	0	0.0125(2)	
As1*a*	0	0.6911(1)	−½	0.0115(5)	
As2	0.28247(9)	0.38891(9)	0.6400(2)	0.0121(4)	
As2*a*	0.2806(1)	0.61845(9)	0.1327(2)	0.0147(4)	
O1	0.0353(6)	0.2360(6)	0.219(1)	0.013(2)	
O1*a*	0.0351(6)	0.7636(7)	−0.273(1)	0.015(2)	
O2	0.1169(1)	0.3966(3)	0.0186(2)	0.014(2)	
H2	0.09440	0.45940	0.01040	0.017	
O2*a*	0.1164(1)	0.6087(3)	−0.4805(2)	0.019(2)	
H2*a*	0.09650	0.54600	−0.47540	0.023	
O3	0.3529(1)	0.3284(3)	0.8811(2)	0.014(2)	
O3*a*	0.3397(2)	0.6815(3)	0.3688(2)	0.015(2)	
O4	0.1315(2)	0.4111(3)	0.5842(2)	0.017(2)	
H4	0.11680	0.47560	0.56500	0.021	
O4*a*	0.1317(2)	0.5934(3)	0.0819(2)	0.017(2)	
H4*a*	0.12140	0.52840	0.08760	0.020	
O5	0.2873(2)	0.3176(3)	0.4402(2)	0.019(2)	
O5*a*	0.2869(2)	0.6947(3)	−0.0682(2)	0.011(2)	
O6	0.3533(2)	0.5104(3)	0.6701(2)	0.015(1)	
O6*a*	0.3531(2)	0.5051(3)	0.1432(2)	0.017(1)	

not involved oxygen atoms, which form the walls of the channel 2. Almost perfectly in the canter of the common base are situated Cd2 and Cd2*a* atoms, alternatively along [0 0 1] in $[A2']_{2b}$ and $[A2'a]_{2a}$ sites, respectively (Fig. 5).

The same structure can by alternatively described as a structure, which hosts two type of layers denoted as I and II, which are parallel to the (1 0 0) plane (Fig. 6). The layer I is composed of the $[(As1O_4)_{0.5}(As1O_2(OH)_2)_{0.5}]^{2-}$ tetrahedra, which act as a bridges connecting adjacent $M1O_4(OH_{0.5})_2$ octahedra *via* two symmetry equivalents of O1 forming an octahedral–tetrahedral chain along *c*-axis. In the same way $M1aO_4(OH_{0.5})_2$ octahedra with the $[(As1aO_4)_{0.5}(As1aO_2(OH)_2)_{0.5}]^{2-}$ tetrahedra generate similar chains. They are linked in double chains with very strong hydrogen bonds [$A\cdots D$ = 2.447–2.494 Å in **1** and 2.477–2.488 Å in **2**] situated in channels 1 and involving all H2, H2*a*, H4 and H4*a* atoms. The double chains are further linked by Cd2 and Cd2*a* atoms located between double chains in channels 2 and linking them in a layer I (Fig. 6a).

The adjacent layers I are separated from each other by the layers II, composed of edge-sharing $M2M2aO_8(OH_{0.5})_2$ octahedral pairs linked by $[(As2O_4)_{0.5}(As2O_3(OH))_{0.5}]^{2.5-}$ and $[(As2aO_4)_{0.5}(As2aO_3(OH))_{0.5}]^{2.5-}$ tetrahedra. The pairs are oriented parallel to each other along the *c*-axis, while they have a zigzag arrangement along the *b*-axis. In these layers each tetrahedra are linked through their vertices to four *M*2 in the same layer II, two *M*1 from layer I and two Cd atoms in the channel 2 (Fig. 6b).

3.2.1. Octahedral $[M1]_{2b}$, $[M1a]_{2a}$, $[M2]_{4c}$ and $[M2a]_{4c}$ sites

The 6-coordinated M^{2+} cations form four distinct octahedra: $M1O_4(OH_{0.5})_2$, $M1aO_4(OH_{0.5})_2$, $M2O_5(OH_{0.5})$ and $M2aO_5(OH_{0.5})$. In both structures the general $[M2]_{4c}$ and $[M2a]_{4c}$ sites are occupied

Table 6
Anisotropic displacement parameters for **2** with estimated standard deviation in parentheses. The anisotropic displacement parameters are defined as: $\exp[-2\pi^2\sum_{i=1}^{3}\sum_{j=1}^{3}U_i a_i^* a_j^* h_i h_j]$.

Atom	U_{11}	U_{22}	U_{33}	U_{23}	U_{13}	U_{12}
Cd2/Cd2*a*	0.0178(6)	0.072(2)	0.0163(6)	0	0.0041(5)	0
Mg1/Cd1	0.019(2)	0.021(2)	0.011(2)	0	0.003(1)	0
Mg1*a*/Cd1*a*	0.019(2)	0.015(3)	0.014(2)	0	0.011(2)	0
Mg2	0.012(2)	0.008(3)	0.005(2)	0.001(2)	0.005(2)	0.001(2)
Mg2*a*	0.012(2)	0.009(3)	0.007(2)	0.002(2)	0.003(2)	0.004(2)
As1	0.016(1)	0.013(1)	0.0063(9)	0	0.0011(8)	0
As1*a*	0.016(1)	0.010(1)	0.0080(9)	0	0.0047(7)	0
As2	0.0181(7)	0.0088(8)	0.0084(7)	−0.0009(5)	0.0040(5)	0.0000(5)
As2*a*	0.0200(7)	0.0168(9)	0.0083(7)	−0.0016(5)	0.0066(5)	−0.0012(5)
O1	0.014(3)	0.017(5)	0.009(4)	0.000(3)	0.006(3)	0.000(3)
O1*a*	0.017(3)	0.013(4)	0.016(4)	−0.006(4)	0.007(3)	0.002(4)
O2	0.016(4)	0.010(4)	0.014(4)	0.006(4)	0.004(3)	0.007(4)
O2*a*	0.023(4)	0.012(5)	0.026(4)	0.005(4)	0.014(3)	0.007(4)
O3	0.020(4)	0.019(5)	0.005(4)	0.004(3)	0.008(3)	0.003(3)
O3*a*	0.024(4)	0.010(5)	0.005(3)	−0.003(3)	0.000(3)	−0.004(3)
O4	0.012(4)	0.017(5)	0.021(4)	0.007(4)	0.005(3)	0.010(4)
O4*a*	0.022(4)	0.013(4)	0.017(3)	0.001(4)	0.010(3)	0.007(4)
O5	0.019(4)	0.025(4)	0.006(4)	−0.005(4)	−0.001(3)	0.000(4)
O5*a*	0.021(4)	0.004(4)	0.007(4)	−0.003(3)	0.004(3)	−0.001(4)
O6	0.016(3)	0.012(4)	0.010(3)	0.002(3)	−0.003(2)	0.009(4)
O6*a*	0.021(3)	0.016(4)	0.020(3)	0.002(4)	0.012(3)	0.014(4)

Table 7
Selected bond lengths in **1** and **2**.

$Cd_{1.16}Zn_{2.34}(AsO_4)_{1.5}(HAsO_4)(H_2AsO_4)_{0.5}$ (**1**)				$Cd_{0.74}Mg_{2.76}(AsO_4)_{1.5}(HAsO_4)(H_2AsO_4)_{0.5}$ (**2**)			
Cd2—O1*a*(×2)	2.94(1)	Zn2*a*—O1*a*	2.115(5)	Cd2—O1*a*(×2)	3.37(3)	Mg2*a*—O1*a*	2.099(8)
Cd2—O3*a*(×2)	3.156(8)	Zn2*a*—O2	2.135(2)	Cd2—O3*a*(×2)	2.78(2)	Mg2*a*—O2	2.111(4)
Cd2—O5(×2)	3.132(7)	Zn2*a*—O3	2.119(2)	Cd2—O5(×2)	3.40(2)	Mg2*a*—O3	2.105(4)
Cd2—O6(×2)	2.501(2)	Zn2*a*—O5	2.116(2)	Cd2—O6(×2)	2.446(2)	Mg2*a*—O5	2.103(4)
Cd2—O6*a*(×2)	2.403(2)	Zn2*a*—O5*a*	2.135(3)	Cd2—O6*a*(×2)	2.366(2)	Mg2*a*—O5*a*	2.110(6)
Average <Cd2—O>	<2.83>	Zn2*a*—O6*a*	2.050(3)	Average <Cd2—O>	<2.87>	Mg2*a*—O6*a*	2.078(6)
Cd2*a*—O1(×2)	2.963(7)	Average <Zn2*a*—O>	<2.11>	Cd2*a*—O1(×2)	3.178(8)	Average <Mg2*a*—O>	<2.10>
Cd2*a*—O3(×2)	2.938(3)	As1—O1(×2)	1.678(5)	Cd2*a*—O3(×2)	2.737(4)	As1—O1(×2)	1.672(7)
Cd2*a*—O5*a*(×2)	3.286(3)	As1—O2(×2)	1.706(2)	Cd2*a*—O5*a*(×2)	3.372(3)	As1—O2(×2)	1.709(2)
Cd2*a*—O6(×2)	2.268(1)	Average <As1—O>	<1.69>	Cd2*a*—O6(×2)	2.237(2)	Average <As1—O>	<1.69>
Cd2*a*—O6*a*(×2)	2.375(1)	As1*a*—O1*a*(×2)	1.669(5)	Cd2*a*—O6*a*(×2)	2.316(2)	As1*a*—O1*a*(×2)	1.682(7)
Average <Cd2*a*—O>	<2.77>	As1*a*—O2*a*(×2)	1.694(2)	Average <Cd2*a*—O>	<2.77>	As1*a*—O2*a*(×2)	1.695(2)
Zn1/Cd1—O1(×2)	2.245(6)	Average <As1*a*—O>	<1.68>	Mg1/Cd1—O1(×2)	2.169(7)	Average <As1*a*—O>	<1.69>
Zn1/Cd1—O3*a*(×2)	2.257(2)	As2—O3	1.678(2)	Mg1/Cd1—O3*a*(×2)	2.162(3)	As2—O3	1.690(2)
Zn1/Cd1—O4(×2)	2.294(2)	As2—O4	1.707(1)	Mg1/Cd1—O4(×2)	2.177(4)	As2—O4	1.722(2)
Average <*M*1—O>	<2.27>	As2—O5	1.673(2)	Average <*M*1—O>	<2.17>	As2—O5	1.633(2)
Zn1*a*/Cd1*a*—O1*a*(×2)	2.216(5)	As2—O6	1.667(3)	Mg1*a*/Cd1*a*—O1*a*(×2)	2.122(7)	As2—O6	1.705(3)
Zn1*a*/Cd1*a*—O3(×2)	2.216(2)	Average <As2—O>	<1.68>	Mg1*a*/Cd1*a*—O3(×2)	2.147(3)	Average <As2—O>	<1.69>
Zn1*a*/Cd1*a*—O4*a*(×2)	2.173(2)	As2*a*—O3*a*	1.669(2)	Mg1*a*/Cd1*a*—O4*a*(×2)	2.107(3)	As2*a*—O3*a*	1.665(2)
Average <*M*1*a*—O>	<2.20>	As2*a*—O4*a*	1.736(2)	Average <*M*1*a*—O>	<2.13>	As2*a*—O4*a*	1.711(2)
Zn2—O1	2.142(6)	As2*a*—O5*a*	1.672(2)	Mg2—O1	2.108(8)	As2*a*—O5*a*	1.679(2)
Zn2—O2*a*	2.102(2)	As2*a*—O6*a*	1.681(2)	Mg2—O2*a*	2.068(4)	As2*a*—O6*a*	1.643(3)
Zn2—O3*a*	2.070(2)	Average <As2*a*—O>	<1.69>	Mg2—O3*a*	2.056(3)	Average <As2*a*—O>	<1.67>
Zn2—O5	2.135(3)			Mg2—O5	2.085(6)		
Zn2—O5*a*	2.150(2)			Mg2—O5*a*	2.099(3)		
Zn2—O6	2.064(3)			Mg2—O6	2.045(6)		
Average <Zn2—O>	<2.11>			Average <Mg2—O>	<2.08>		

Table 8
Results of bond-valence sum $\sum v_{ij}$ (valence units) calculations for **1** and **2**.

		Cd2	Cd2*a*	*M*1	*M*1*a*	*M*2	*M*2*a*	As1	As1*a*	As2	As2*a*	$\sum v_{ij}$
1	O1		0.045/0.090	0.374/0.748		0.306		1.272/2.544				1.997
	O1*a*	0.013/0.026			0.333/0.666		0.329		1.303/2.606			1.978
	O2						0.312	1.179/2.358				1.491
	O2*a*					0.341			1.218/2.436			1.559
	O3		0.048/0.096		0.333/0.666		0.326			1.272		1.979
	O3*a*	0.007/0.014		0.362/0.724		0.372					1.303	2.044
	O4			0.329/0.658						1.176		1.505
	O4*a*				0.374/0.748						1.087	1.461
	O5	0.008/0.016				0.312	0.328			1.289		1.937
	O5*a*		0.019/0.038			0.300	0.312				1.293	1.924
	O6	0.043/0.085	0.294/0.588			0.378				1.310		2.025
	O6*a*	0.056/0.111	0.220/0.440				0.393				1.262	1.931
	$\sum v_{ij}$	0.252	1.252	2.130	2.080	2.009	2.000	4.902	5.042	5.047	4.945	
2	O1		0.029/0.058	0.345/0.690		0.326		1.293/2.586				1.993
	O1*a*	0.002/0.004			0.352/0.704		0.334		1.258/2.516			1.946
	O2						0.323	1.170/2.340				1.493
	O2*a*					0.363			1.215/2.430			1.578
	O3		0.095/0.190		0.329/0.658		0.328			1.231		1.983
	O3*a*	0.009/0.018		0.352/0.704		0.375					1.317	2.053
	O4			0.338/0.676						1.129		1.467
	O4*a*				0.367/0.734						1.163	1.530
	O5	0.002/0.004				0.347	0.330			1.436		2.115
	O5*a*		0.017/0.034			0.334	0.314				1.269	1.934
	O6	0.022/0.044	0.368/0.736			0.386				1.182		1.958
	O6*a*	0.028/0.056	0.297/0.594				0.353				1.398	2.076
	$\sum v_{ij}$	0.126	1.612	2.070	2.096	2.131	1.982	4.926	4.946	4.978	5.147	

Table 9
Hydrogen bonding geometry in structures of **1** and **2**.

D—H···*A*	*D*—H (Å)	H···*A* (Å)	*D*···*A* (Å)	*D*—H···*A* (°)
$Cd_{1.16}Zn_{2.34}(AsO_4)_{1.5}(HAsO_4)(H_2AsO_4)_{0.5}$ (**1**)				
O2—H2···O4*a*	0.82	1.75	2.494(4)	149.5
O4—H4···O2*a*	0.82	1.63	2.447(4)	174.2
O2*a*—H2*a*···O4	0.82	1.72	2.447(4)	147.3
O4*a*—H4*a*···O2	0.82	1.72	2.494(4)	156.4
$Cd_{0.74}Mg_{2.76}(AsO_4)_{1.5}(HAsO_4)(H_2AsO_4)_{0.5}$ (**2**)				
O2—H2···O4*a*	0.82	1.74	2.477(4)	148.0
O4—H4···O2*a*	0.82	1.68	2.488(4)	167.3
O2*a*—H2*a*···O4	0.82	1.74	2.488(4)	151.6
O4*a*—H4*a*···O2	0.82	1.70	2.477(4)	158.0

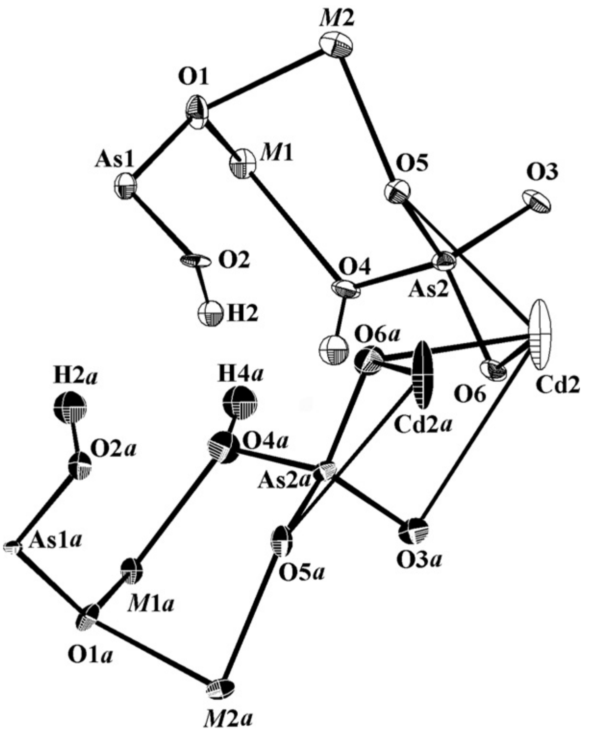

Fig. 2. The asymmetric unit with the atom-numbering scheme. Displacement ellipsoids are plotted at the 90% probability level. The long Cd—O bonds are shown as thin lines. White ellipsoids represent the asymmetric unit for alluaudite in *C*2/*c* space group. The Zn in **1** and Mg in **2** atoms fill two octahedral *M*2 and *M*2*a* sites, while *M*1 and *M*1*a* (*M*1 = Cd/Zn and Cd/Mg in **1** and **2**, respectively) are mixed octahedral sites.

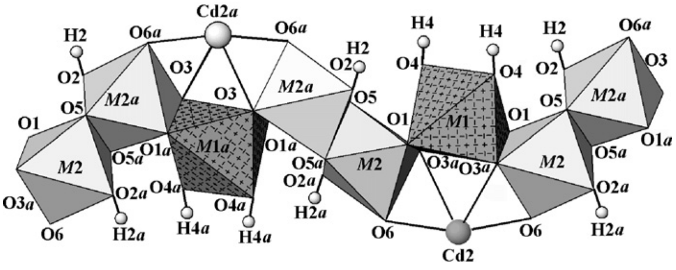

Fig. 3. The infinite octahedral chain of edge-sharing $M2M2aO_8(OH_{0.5})_2$ pairs (grey) linked by $M1O_4(OH_{0.5})_2$ and $M1aO_4(OH_{0.5})_2$ octahedra (hachured dark grey) in the projection nearly parallel to the *ab*-plane (*a*-axis is horizontal and *b*-axis is vertical).

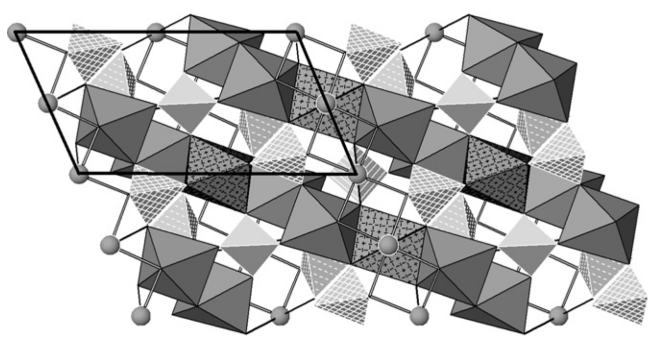

Fig. 4. Projection of the structure parallel to the (0 1 0) plane (*a*-axis is horizontal). The octahedral chains (dark grey and hachured dark grey) running parallel to (1 0 1) planes in one layer with arsenate groups (white hachured light grey tetrahedra) and Cd atoms (sphere). Hydrogen atoms were neglect because of clarity.

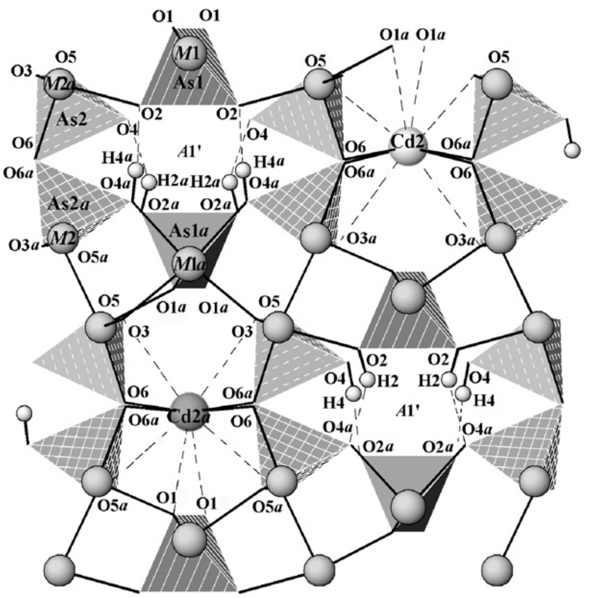

Fig. 5. The cross-section of the channels along [0 0 1] (*a*-axis is horizontal) with Cd and H atoms in channels 2 and 1, respectively. In both channel 1 presented in a figure, the half of hydrogen atoms is arbitrary omitted in order to illustrate their half-occupied positions.

by Zn in **1** and Mg in **2**, while special $[M1]_{2b}$ and $[M1a]_{2a}$ are mixed sites occupied by Cd/Zn and Cd/Mg in **1** and **2**, respectively.

Average *M*2—O and *M*2*a*—O bond lengths are 2.111(3) and 2.112(3) Å in **1** and 2.077(4) and 2.101(5) Å in **2,** which are in good agreement with calculated values (2.12 and 2.10 Å, respectively) for the sum of effective ionic radii of the Zn^{2+} and O^{2-} ions in **1** and Mg^{2+} and O^{2-} ions in **2** [60]. Average *M*1—O and *M*1*a*—O lengths are a bit longer than *M*2—O and *M*2*a*—O, *i.e.* 2.265(3) and 2.202(3) Å in **1** and 2.169(4) and 2.125(4) Å in **2**, respectively, indicating the incorporation of the larger Cd cation. The occupancy factors for $[M1]_{2b}$ and $[M1a]_{2a}$ sites show the different cation distributions: $Cd1_{0.86}/Zn1_{0.14}$, $Cd1a_{0.46}/Zn1a_{0.54}$ in **1** and $Cd1_{0.33}/Mg1_{0.67}$, $Cd1a_{0.16}/Mg1a_{0.84}$ in **2** (calculated bond lengths are 2.27, 2.20, 2.23, 2.15 Å, respectively).[1]

3.2.2. Tetrahedral $[X1]_{2a}$, $[X1a]_{2b}$, $[X2]_{4c}$ and $[X2a]_{4c}$ sites and hydrogen bonding

The four crystallographically non-equivalent $[(As1O_4)_{0.5}(As1O_2(OH)_2)_{0.5}]^{2-}$, $[(As1aO_4)_{0.5}(As1aO_2(OH)_2)_{0.5}]^{2-}$, $[(As2O_4)_{0.5}(As2O_3(OH))_{0.5}]^{2.5-}$ and $[(As2aO_4)_{0.5}(As2aO_3(OH))_{0.5}]^{2.5-}$ tetrahedra are all protonated. Two O2 and two O2*a* atoms, of the $[(As1O_4)_{0.5}(As1O_2(OH)_2)_{0.5}]^{2-}$ and $[(As1aO_4)_{0.5}(As1aO_2(OH)_2)_{0.5}]^{2-}$ groups are bonded to atoms H2 and H2*a*, while the O4 and O4*a*, of the $[(As2O_4)_{0.5}(As2O_3(OH))_{0.5}]^{2.5-}$ and $[(As2aO_4)_{0.5}(As2aO_3(OH))_{0.5}]^{2.5-}$ groups, are bonded to atoms H4 and H4*a*, respectively (Fig. 5). All H atoms are located on half-occupied general positions somewhat off the $[A1']_{2b}$ and $[A1'a]_{2a}$ sites, so that only half of the sites are occupied by OH and another half are occupied by O. Accordingly, OH groups are statistically distributed among four positions within the channel 1 and are involved in a similarly strong hydrogen bonds.

Due to the symmetry requirements $[(As1O_4)_{0.5}(As1O_2(OH)_2)_{0.5}]^{2-}$ and $[(As1aO_4)_{0.5}(As1aO_2(OH)_2)_{0.5}]^{2-}$ tetrahedra are doubly protonated (two symmetry equivalents of O2 and O2*a*, respectively) and act as hydrogen bond donors to the oxygens O4*a*

---

[1] *e.i.r.* for 6-coordinated Zn^{2+}, Mg^{2+}, and Cd^{2+} are 0.740, 0.720, and 0.950 Å, respectively.

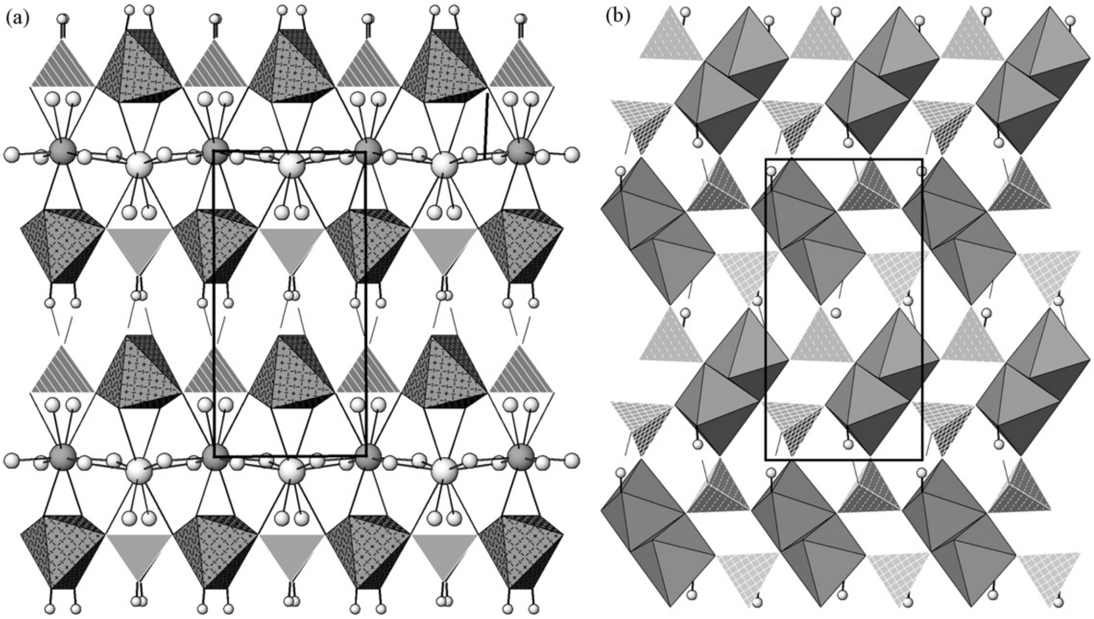

Fig. 6. Projection of a single polyhedral layer I (a) and layer II (b) parallel to the (1 0 0) plane (*b*-axis is vertical). Hachured dark grey octahedra represent the mixed site coordination polyhedra, while dark grey are for $M2M2aO_8(OH_{0.5})_2$ pairs. Tetrahedra represent $[(AsO_4)_{0.5}(AsO_3(OH))_{0.5}]^{2.5-}$ and $[(AsO_4)_{0.5}(AsO_2(OH)_2)_{0.5}]^{2-}$ groups. The largest circles indicate Cd atoms (light grey for Cd2 and dark grey for Cd2*a*) in channel 2, the middle are for oxygen, whereas the smallest circles are for hydrogen atoms. Some hydrogen atoms are arbitrary omitted in order to illustrate their statistical distribution.

and O4 in one half, and as single hydrogen bond acceptors from another OH groups (O4H4 and O4*a*H4*a*, respectively) in the second half of unit cells.

Similarly, the already mentioned OH groups (O4H4 and O4*a*H4*a*) act as hydrogen bond donors toward the oxygens O2*a* and O2, in one half, and as single hydrogen bond acceptors from O2*a*H2*a* and O2H2, respectively, in the second half time (Fig. 5). Expectedly, the As—OH bond distances are slightly elongated in comparison to the other As—O bonds in tetrahedra (see Table 7).

3.2.3. Ten-coordinated $[A2']_{2b}$ and $[A2'a]_{2a}$ sites

Both Cd2 and Cd2*a* atoms have ten O ligands, four at shorter and six at longer distance in both structures (Table 7). The $\mathrm{Cd2O_{10}}$ and $\mathrm{Cd2}a\mathrm{O_{10}}$ polyhedra are interconnected in chains running in the *c*-direction, where every $\mathrm{Cd2O_{10}}$ polyhedron shares two opposite edges with neighbouring $\mathrm{Cd2}a\mathrm{O_{10}}$ polyhedra.

The symmetry of the both Cd sites and their coordination polyhedra are 2, which place the two Cd atoms on neighbouring two-fold axes. Two nearest Cd atoms (Cd2 and Cd2*a*) are bridged by two O atoms (O6 and O6*a*) at maximum distances of 2.5 Å. With these closest O atoms (two symmetry-equivalents of O6 and two of O6*a*), Cd2 and Cd2*a* lie in an almost perfectly planar plane normal to the *b*-axis which is the central part of the chain (Figs. 4 and 5). The Cd2···Cd2*a* distance along the chain extension is 3.4550(3) Å in **1** and 3.3744(5) Å in **2**, which is longer than the sum of the Van der Waals radii [3.16 Å for $2 \times r_{\mathrm{Cd}}$] [61].

Assuming O atoms at longer distances the $\mathrm{CdO_{10}}$ coordination polyhedra can be described as containing two adjacent parts: a distorted trigonal prism (housing the four shortest and two longer bonds) and a highly irregular square antiprism sharing its square base (with two symmetry-equivalents of O6 and two of O6*a* in vertices) with one lateral face of the trigonal prism. The $\mathrm{CdO_{10}}$ polyhedra are characterized by average Cd2—O and Cd2*a*—O bond lengths of 2.827(6) Å for $\mathrm{Cd2_{0.21}\square_{0.79}}$ and 2.766(3) Å for $\mathrm{Cd2}a_{0.79}\square_{0.21}$ in **1** and 2.872(3) Å for $\mathrm{Cd2_{0.10}\square_{0.90}}$ and 2.768(8) Å for $\mathrm{Cd2}a_{0.90}\square_{0.10}$ in **2**, respectively.

3.2.4. Bond valence calculations

The bond valence values for cadmium atoms situated in channel 2 are lower than 1.8 v.u., indicating that these sites are significantly underbonded, partly due to incomplete occupation of these sites, and structure disorder.

The bond valence sums for the oxygen atoms, which are not involved in hydrogen bonding, have values in very good agreement to assumed and range from 1.92 to 2.04 v.u. in **1** and 1.93 to 2.12 v.u. in **2**. Oppositely, values for those oxygen atoms involved in hydrogen bonding range from 1.46 to 1.56 v.u. in **1** and 1.47–1.58 v.u. in **2**. Having in mind the fact that O2, O2*a*, O4, and O4*a* are alternately hydrogen bonding donors and acceptors to one another, bond valence values for both compounds are very well balanced. Bond valence sum calculations for both **1** and **2** alluaudites are shown in Table 8.

3.3. FT-IR analysis results

In order to investigate the hydroxyl group content of the title compounds polarized single-crystal FT-IR spectra of **1** and **2** were recorded. The presence of hydrogen bonding can be detected by infrared spectroscopy in the domains of the OH^- stretching modes. Due to the strong absorption bands under 1000 $\mathrm{cm^{-1}}$ could not be analysed (there was not enough sample for the KBr micropallet method). However, the distinct frequency ranges for **1** and **2** may be assigned as follows: the spectral region between 3500 and 1000 $\mathrm{cm^{-1}}$ shows a peculiar increase in “background absorption” (Figs. 7a and b), which is a typical feature of compounds with very short, *i.e.*, very strong hydrogen bonds (*e.g.*, $Sr_5(As_2O_7)_2(AsO_3OH)$ [62]; $Sr_4Cu_3(AsO_4)_2(AsO_3OH)_4\ 3H_2O$ [42] and references therein), which is the case with both **1** and **2**. Because of the broad band shape, As—O tetrahedral stretching vibrations and lattice modes are superimposed in the low-energy region of the spectrum. The infrared spectrum clearly shows the presence of broad O—H stretching and bending vibrations centred around 3236, 2300/1310 $\mathrm{cm^{-1}}$ and 3210, 2390/1390 $\mathrm{cm^{-1}}$ for **1** and **2** respectively [63]. According to the d–ν correlation for hydrogen bonds

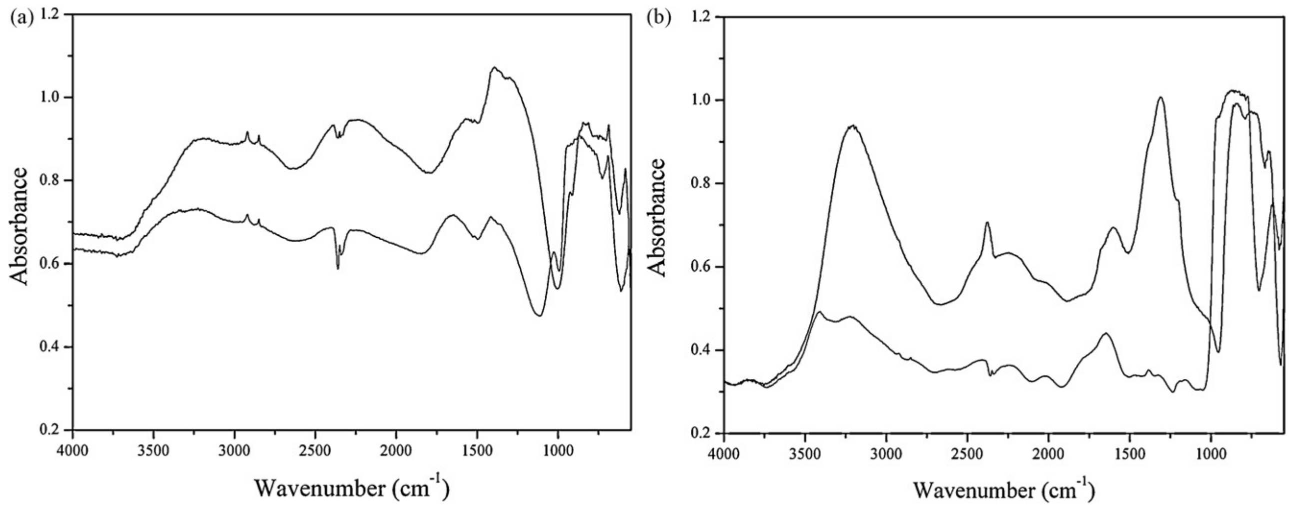

Fig. 7. Polarized single-crystal FT–IR spectra of **1** (a) and **2** (b). O—H stretching bands can be observed in one of polarized spectra (when polarization beam was parallel to the elongation of the crystal), whereas they are of low intensity in the other polarization direction (perpendicular to the elongation of the crystal).

this wavenumbers are in very good agreement with the refined H···O bond lengths [64]. Bands around 3200 cm^{-1} agree well with H···O bond lengths around 1.73 Å, and bands around 2300 cm^{-1} are in good agreement with H···O bond lengths around 1.62 Å.

4. Conclusion

This research has confirmed that synthesis of divalent cation arsenates with cadmium by low-temperature hydrothermal method can yield novel structure types with interesting crystal-chemical properties, such as short hydrogen bond lengths, where oxygen atoms are alternately hydrogen bonding donors and acceptors to each other.

Very probably the twinning and incorporation of Cd/Zn in **1** and Cd/Mg in **2** results in the change of symmetry from $C2/c$ to $C2$, which is a subgroup of the space group $C2/c$. This transition to the subgroup $C2$ reduced symmetry, thus causing a splitting of general position 8*f* into two positions of multiplicity of 4 and one special 4*e* into two with multiplicities of 2 allowing a distortion of the structure.

In **1** and **2** structures, Cd ions partly occupy both $[A2']_{2b}+[A2'a]_{2a}$ disordered sites in channels running along *c*-axis, while Zn in **1** and Mg in **2** fill two non-mixed octahedral $[M2]_{4c}+[M2a]_{4c}$ sites, and together with Cd ions form two mixed octahedral sites $[M1]_{2b}+[M1a]_{2a}$. Moreover, the lattice volume increases with the increase of concentration of the largest cation, Cd^{2+}.

This research showed that metal-arsenates are not fully crystallographically defined. Additional investigation of this system would lead to full knowledge, which topologies are likely to form under which conditions (*e.g.*, temperature, pressure, ratios of ionic radii, pH, ...). Moreover, facts obtained in this study might be useful to the phosphates, vanadates and silicates with analogous structure. Furthermore, permanent research of arsenic containing compounds should be carried out because of potentially appealing features of these compounds and since arsenic is recognized to be one of the most lethal chemical elements for our environment. Therefore, this is the main reason why arsenates are not examined in a satisfactory manner and thus, their crystal-chemical characteristics are frequently indefinite. Authors of this study have hope that this is just an introduction to a thorough research which will be the subject of our future work.

Acknowledgements

Financial support of the Austrian Science Foundation (FWF) (Grant T 300-N19) and the Ministry for Education and Science of the Republic of Serbia (Project Nos. III45007, OI172004 and OI176016) are gratefully acknowledged.

References

[1] D. Antenucci, G. Miehe, P. Tarte, W.W. Schmahl, A.-M. Fransolet, Eur. J. Mineral. 5 (1993) 207–213.
[2] M. Auernhammer, H. Effenberger, G. Hentschel, T. Reinecke, E. Tillmanns, Miner. Petrol. 48 (1993) 153–166.
[3] T.E. Warner, W. Milius, J. Mainer, J. Solid State Chem. 106 (1993) 301–309.
[4] S. Boudin, A. Grandin, M.M. Borel, A. Leclaire, B. Raveau, J. Solid State Chem. 110 (1994) 43–49.
[5] K.-H. Lii, P.-F. Shih, Inorg. Chem. 33 (1994) 3028–3031.
[6] D. Antenucci, A.-M. Fransolet, G. Miehe, P. Tarte, Eur. J. Mineral. 7 (1995) 175–181.
[7] F. Leroux, A. Mar, C. Payen, D. Guyomard, A. Verbaere, Y. Piffard, J. Solid State Chem. 115 (1995) 240–246.
[8] F. Leroux, A. Mar, D. Guyomard, Y. Pittard, J. Solid State Chem. 117 (1995) 206–212.
[9] K.-H. Lii, J. Ye, J. Solid State Chem. 131 (1997) 131–137.
[10] M.B. Korzenski, G.L. Schimek, J.W. Kolis, Solid State Chem. 139 (1998) 152–160.
[11] F. Hatert, P. Keller, F. Lissner, D. Antenucci, A.-M. Fransolet, Eur. J. Mineral. 12 (2000) 847–857.
[12] N. Chouaibi, A. Daidouh, C. Pico, A. Santrich, M.L. Veiga, J. Solid State Chem. 159 (2001) 46–50.
[13] N. Stock, G.D. Stucky, A.K. Cheetham, J. Phys. Chem. Solids 62 (2001) 1457–1467.
[14] B. Ayed, M. Krifa, A. Haddad, Acta Crystallogr. C 58 (2002) i98–i100.
[15] C. Durio, A. Daidouh, N. Chouaibi, C. Pico, M.L. Veiga, J. Solid State Chem. 168 (2002) 208–216.
[16] F. Hatert, D. Antenucci, A.-M. Fransolet, M.L. Duyckaerts, J. Solid State Chem. 163 (2002) 194–201.
[17] A. Guesmi, A. Driss, Acta Crystallogr. C 58 (2002) i16–i17.
[18] B.S. Ridha, J. Tahar, Acta Crystallogr. C 58 (2002) i61–i62.
[19] A. Daidouh, C. Durio, C. Pico, M.L. Veiga, N. Chouaibi, A. Ouassini, Solid State Sci. 4 (2002) 541–548.
[20] F. Hatert, R.P. Hermann, G.J. Long, A.-M. Fransolet, F. Grandjea, Am. Mineral. 88 (2003) 211–222.
[21] M. Hidouri, B. Lajmi, A. Driss, M. Ben Amara, Acta Crystallogr. E 59 (2003) i7–i9.
[22] B. Ayed, A. Haddad, Acta Crystallogr. E 59 (2003) i77–i79.
[23] N. Stock, T. Bein, Solid State Sci. 5 (2003) 1207–1210.
[24] F. Hatert, Miner. Petrol. 81 (2004) 205–217.
[25] F. Hatert, G.J. Long, D. Hautot, A.-M. Fransolet, J. Delwiche, M.J. Hubin-Franskin, F. Grandjean, Phys. Chem. Minerals 31 (2004) 487–506.
[26] M. Hidouri, B. Lajmi, A. Wattiaux, L. Fournes, J. Darriet, M.B. Amara, J. Solid State Chem. 177 (2004) 55–60.
[27] Z.M. Faouzi, A. Driss, J. Tahar, Acta Crystallogr. E 61 (2005) i46–i48.
[28] F. Hartert, L. Rebbouh, R.P. Hermann, A.-M. Fransolet, G.J. Long, F. Grandjean, Am. Mineral. 90 (2005) 653–662.
[29] M. Kacimi, M. Ziyad, F. Hatert, Mater. Res. Bull. 40 (2005) 682–693.
[30] H. Sarp, R. Cerny, Eur. J. Mineral. 17 (2005) 367–373.

[31] F. Hatert, Acta Crystallogr. C 62 (2006) i1–i2.
[32] M.A. Strelkov, M.G. Zhizhin, L.N. Komissarova, J. Solid State Chem. 179 (2006) 3664–3671.
[33] F. Hatert, A.-M. Fransolet, W.V. Maresch, Contrib. Mineral. Petrol. 52 (2006) 399–419.
[34] F. Hatert, J. Solid State Chem. 181 (2008) 1258–1272.
[35] A.H. Abdallah, A. Haddad, Acta Crystallogr. E 64 (2008) i36.
[36] M.A. Cooper, F.C. Hawthorne, N.A. Ball, R.A. Ramik, A.C. Roberts, Can. Mineral. 47 (2009) 1225–1235.
[37] F. Hatert, L. Ottolini, P.S. Beurmann, Contrib. Mineral. Petrol. 161 (2011) 531–546.
[38] M. Rondeux, F. Hatert, Am. Mineral. 95 (2010) 844–852.
[39] K. Trad, D. Carlier, L. Croguennec, A. Wattiaux, M.B. Amara, C. Delmas, Chem. Mater. 22 (2010) 5554–5562.
[40] P.B. Moore, Am. Mineral. 56 (1971) 1955–1975.
[41] T. Đorđević, S. Šutović, J. Stojanović, Lj Karanović, Acta Crystallogr. C 64 (2008) i82–i86.
[42] T. Đorđević, Lj Karanović, J. Solid State Chem. 181 (2008) 2889–2898.
[43] T. Đorđević, Lj Karanović, J. Solid State Chem. 183 (2010) 2835–2844.
[44] J. Stojanović, T. Đorđević, Lj Karanović, Acta Crystallogr. C 64 (2008) i91–i94.
[45] M. Weil, T. Đorđević, C.L. Lengauer, U. Kolitsch, Solid State Sci. 11 (2009) 2111–2117.
[46] J. Stojanović, T. Đorđević, Lj Karanović, Acta Crystallogr. C 66 (2010) i55–i57.
[47] P. Keller, H. Riffel, F. Zettler, H. Hess, Z. Anorg, Allg. Chem. 474 (1981) 123–134.
[48] P. Keller, H.N. Hess, Jb. Miner. Mh. 9 (1988) 395–404.
[49] R.B. Smail, T. Jouini, Acta Crystallogr. C 58 (2002) i61–i62.
[50] A. Assani, M. Saadi, M. Zriouil, L. Ammari, Acta Crystallogr. E 67 (2011) i5.
[51] Bruker-Nonius APEX2 and SAINT-Plus, Bruker AXS Inc., Madison, WI, USA, 2004.
[52] Z. Otwinowski, W. Minor, Meth. Enzymol. 276 (1997) 307.
[53] Z. Otwinowski, D. Borek, W. Majewski, W. Minor, Acta Crystallogr. A 59 (2003) 228.
[54] A. Altomare, M.C. Burla, M. Camalli, G.L. Cascarano, C. Giacovazzo, A. Guagliardi, A.G.G. Moliterni, G. Polidori, R. Spagna, J. Appl. Crystallogr. 32 (1999) 115–119.
[55] G.M. Sheldrick, Acta Crystallogr. A 64 (2008) 112–122.
[56] L.J. Farrugia, J. Appl. Crystallogr. 32 (1999) 837–838.
[57] A.S. Wills, VALIST: Program available from www.CCP14.ac.uk, 2009.
[58] E. Dowty, ATOMS. V. 6.1.: A Complete Program for Displaying Atomic Structures, Shape Software, Kingsport, TN, USA, 1999.
[59] R.X. Fischer, E. Tillmanns, Acta Crystallogr. C 44 (1988) 775–776.
[60] R.D. Shannon, Acta Crystallogr. A 32 (1976) 751–767.
[61] A. Bondi, J. Phys. Chem. 68 (1964) 441–451.
[62] T. Mihajlović, E. Libowitzky, H. Effenberger, J. Solid State Chem. 177 (2004) 3963–3970.
[63] N. Stock, C. Jargstorff, S. Wriedt, Z. Anorg, Allg. Chem. 637 (2001) 572–577.
[64] E. Libowitzky, Mh. Chem. 130 (1999) 1047–1059.